

Supporting Information

Feedback Control for Defect-free Alignment of Colloidal Particles

Yu Gao, Richard Lakerveld *

Department of Chemical and Biological Engineering
The Hong Kong University of Science and Technology
Clear Water Bay, Hong Kong S.A.R
E-mail: kelakerveld@ust.hk

Process flow for fabrication of patterned electrodes

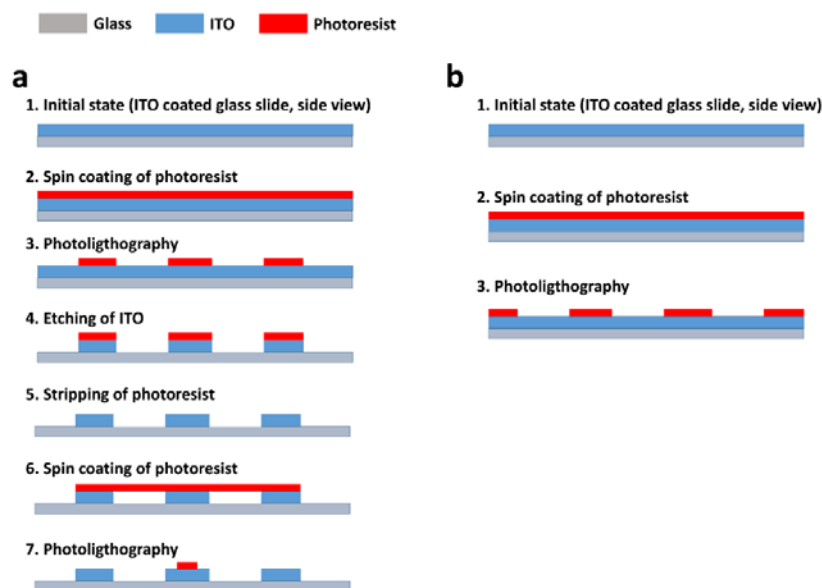


Figure S1. Schematic illustration of the patterned electrode fabrication procedure.

a, For electrode in Figure 2a of the manuscript. **b**, For electrodes in Figure 1a of the manuscript.

Change of order parameter when applying different potential differences in open-loop mode

The order parameter is well capable to track the extent of alignment when changing the potential difference as illustrated in Figure S2. The measurement noise is mainly caused by the Brownian motion of the particles.

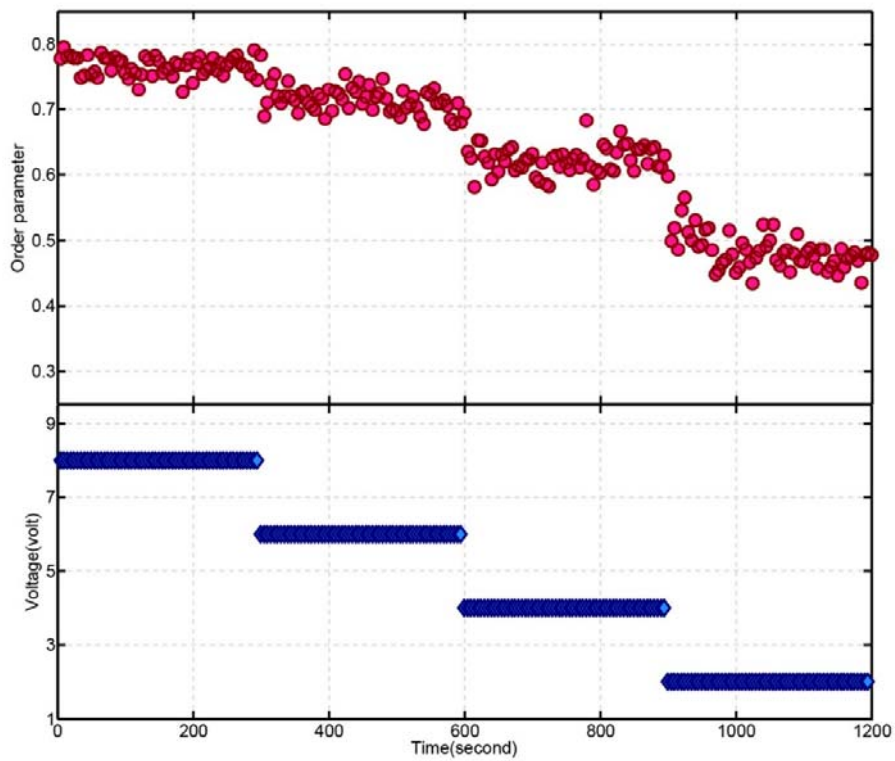


Figure S2. Order parameter as function of time for different voltages (open-loop mode).

Change of order parameter when applying different frequencies in open-loop mode

As shown in Figure S3, the order parameter can also track the extent of alignment when using the frequency as manipulated variable instead of potential difference. However, the system is characterized by a strong non-linear behavior.

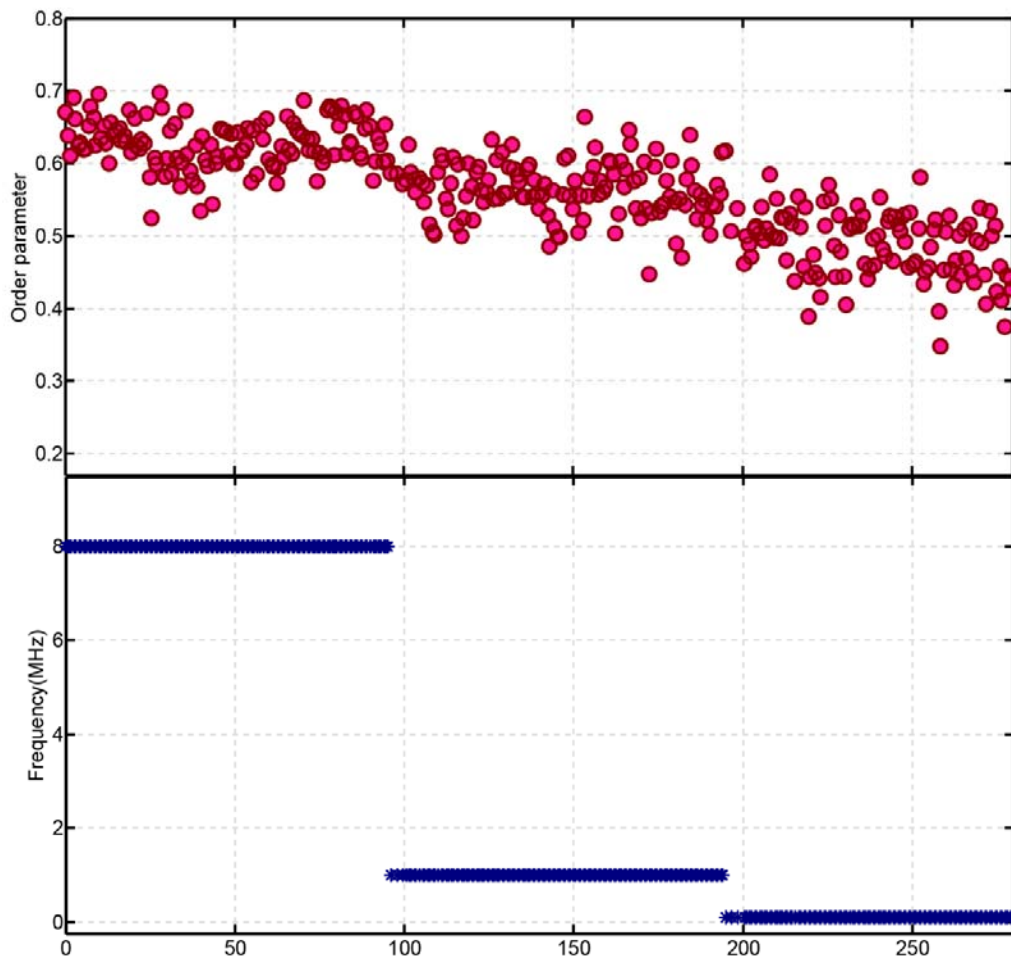


Figure S3. Order parameter as function of time for different frequencies (open-loop mode).

PI control of alignment by manipulating frequency with gain-scheduling strategy

As shown in Figure S4, the order parameter is well controlled around a selected set point when frequency is used as manipulated variable in combination with a gain-scheduling strategy for parameter tuning. However, the range of attainable set points is small due to the low sensitivity of the particle alignment with respect to the frequency for the tested conditions and the limited frequency range of nDEP.

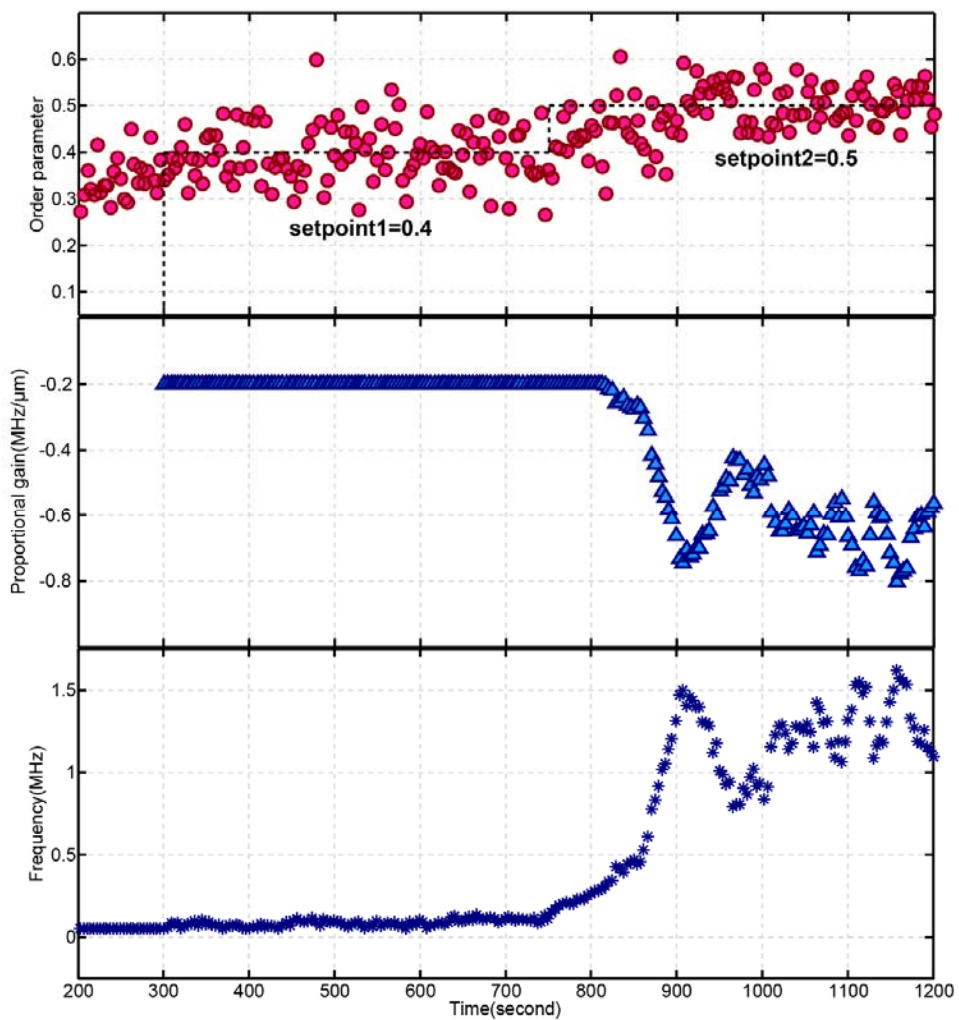


Figure S4. Dynamic change of order parameter, proportional gain and frequency during set point tracking with gain-scheduled PI control.

Analysis of the electrokinetic phenomena in Figure 2b,c of the manuscript

Electro-osmotic flow (EOF) and dielectrophoresis (DEP) are the two main electrokinetic phenomena involved in this study. The EOF is generated by the horizontal component of the electric field around an electrode surface. Such transverse electric field leads to a transverse motion of the ions in the electrical double layer (EDL), which leads to fluid motion induced by electro-osmosis.^[1-4] EOF typically happens at a frequency below 3-5 kHz as for a higher frequency there is not sufficient time for ions to accumulate to form the EDL during each cycle of the applied AC electric field.^[1] DEP is a phenomenon in which a force induced by an electric field acts on a particle polarized in a non-uniform electric field, which results in the attraction of the particle to either a field maximum or minimum.^[5,6] The particle is attracted to an electric field maximum if the particle is more polarized than the medium, which is called positive dielectrophoresis (pDEP). Otherwise, if the particle is attracted to an electric field minimum, the phenomenon is called negative dielectrophoresis (nDEP).

Figure S5 illustrates the norm of the electric field strength obtained from a simulation (COMSOL Multiphysics 5.3) of the electric field around the electrodes that are illustrated in Figure 2a of the manuscript with only a potential applied to the outer ITO electrode stripes. An electric field minimum exists at the center of the cell above the stripe of photoresist that is placed on top of the electrode, which suggests that the density increase observed in the middle of the cells (see Figure 2c of the manuscript) is

driven by nDEP at high frequency. A maximum in field strength occurs near the edges of the ITO electrodes (see Figure S5a). Such particle movement is in principle consistent with pDEP, which attracts the particles to the edges of the outer ITO electrode stripes if the field frequency is compatible with pDEP. However, experimentally it was observed that the particles moved to the center of the outer electrode stripes at the applied frequency instead of to the edges (see Figure S6). Such behavior is more consistent with an EOF-dominated system, which has been observed and investigated by others for similar systems.^[2] Therefore, although pDEP may also occur under those conditions, it is likely that pDEP is not the dominant electrokinetic phenomenon.

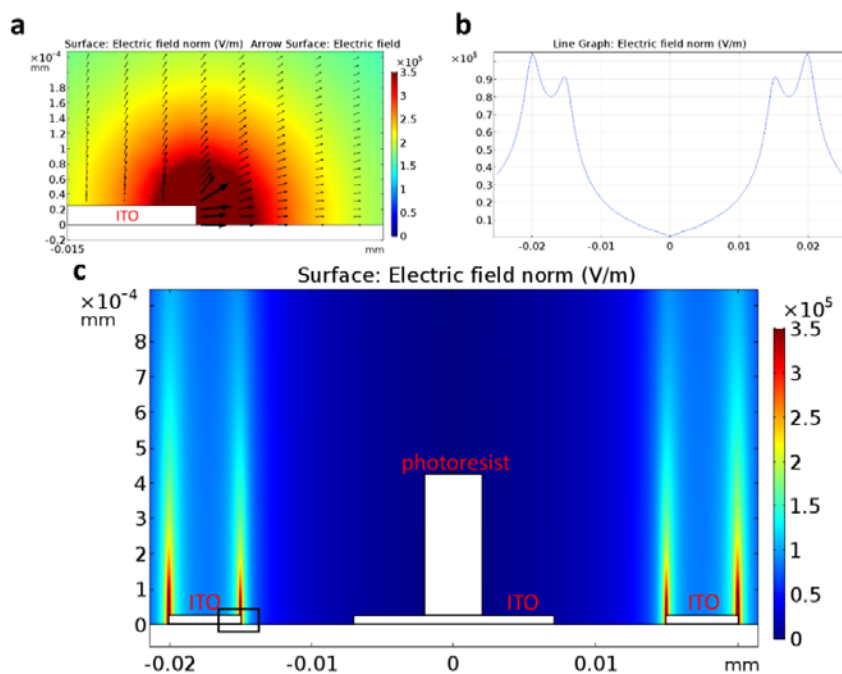


Figure S5. Simulation of the electric field for the electrode design in Figure 2a of the manuscript, with mode of outer ITO electrode being powered on. a, zoom-in at

the square region in **c. b**, 1D distribution of the electric field strength at the height of $1\mu\text{m}$ in **c. c**, 2D map of the electric field strength.

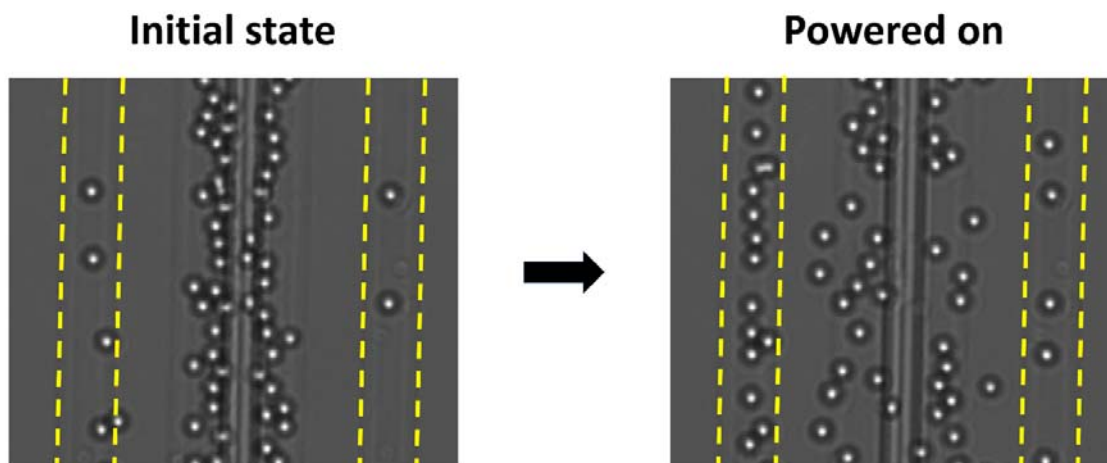


Figure S6. Microscopy image during the procedure when the particle density is decreased on the electrode in Figure 2b of the manuscript. The yellow dotted lines represent the boundary of the outer ITO electrodes, which are powered on during the density control.

Analysis of the noise in density change in Figure 7a of manuscript

From Figure S7a-b, it can be seen that particle P1 is outside the controlled area at point A5, but moves inside the controlled area at point A6. This variation is due to the Brownian motion as the active EOF moves the particle away from the controlled area. Furthermore, it can be seen that the image analysis fails to detect particle P2 at point A5 but succeeds at point A6. In summary, the density increase from A5 to A6 is due to a combination of Brownian motion and the failure of image analysis. Similarly, the increase from A7 to A8 can be explained by Brownian motion.

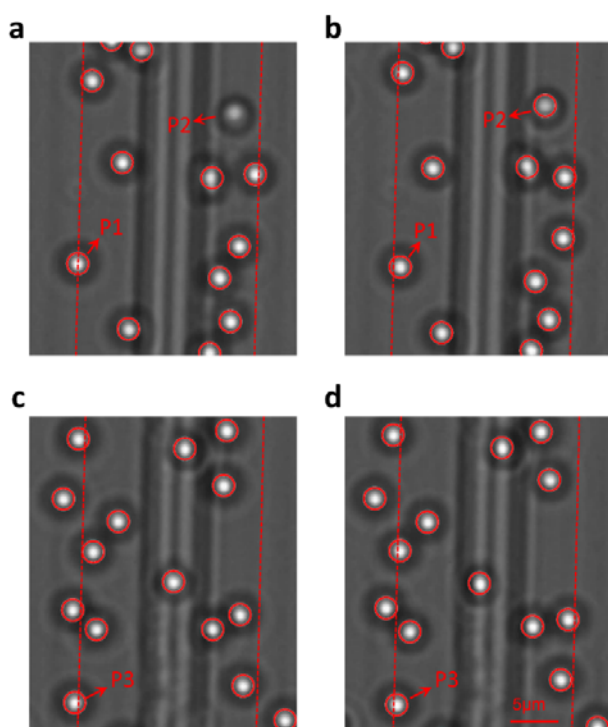


Figure S7. Experimental images corresponding to points A5, A6, A7, and A8 in Figure 7a of the manuscript. a, A5. b, A6. c, A7. d, A8. The four images show only part of the complete microscopy photos for illustrative purposes. The space between the red dashed lines represents the area calculated for particle density. The particles

labeled with red circles are detected by image analysis.

Two different automated mechanisms for switching from density control (“state1”) to transition period (“state2”)

The density change around a switching point between density control (referred to as “state1” in the manuscript) and the transition period (referred to as “state2” in the manuscript) is shown in Figure S8. Cases with different switching mechanisms from different initial densities are included. The advantage of a switch that requires the density to be within the desired range for certain period (“steady-state switch”) is that the possibility of overshoots is reduced, which can be seen when comparing Figure S8a and Figure S8b. Less time is needed when such requirement is absent (“immediate switch“), which can be seen when comparing Figure S8a (Figure S8c) and Figure S8b (Figure S8d).

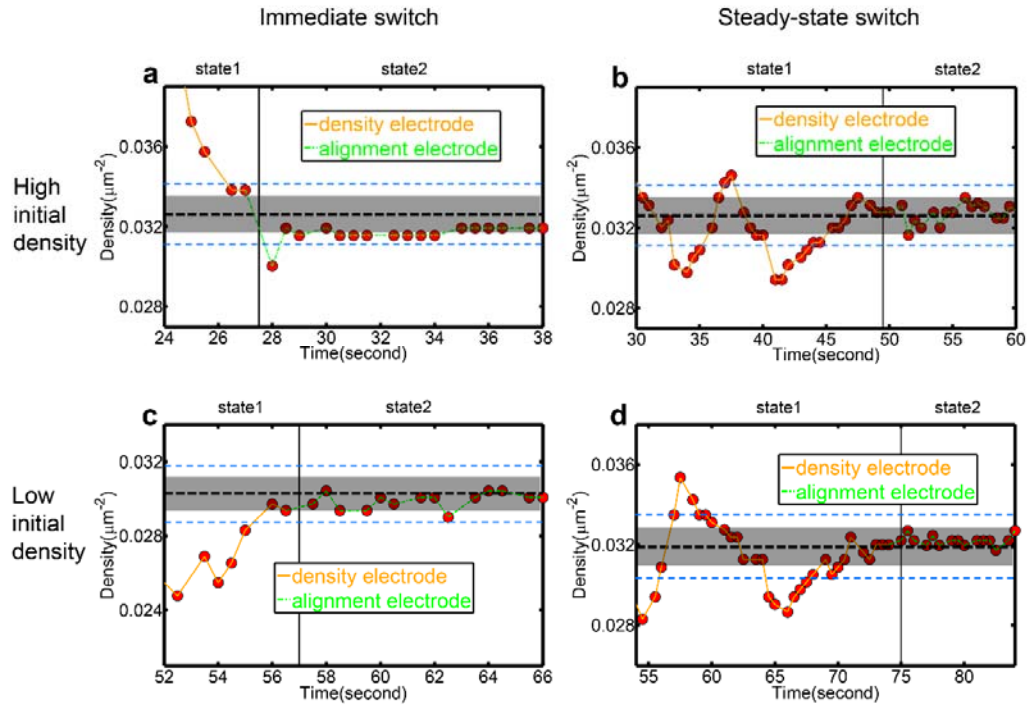


Figure S8. Dynamic change of density for different switching mechanisms and initial densities. **a**, Immediate switching mechanism with high initial density. **b**, Steady-state switching mechanism with high initial density. **c**, Immediate switching mechanism with low initial density. **d**, Steady-state switching mechanism with low initial density. The gray band represents the deadband for density control and the blue dashed lines represents a boundary ($\pm 5\%$ of the set point). The black dashed lines indicate set points. The actuated electrodes for the different periods are illustrated with different colors (i.e., green for the center electrode for alignment and brown for the outer electrode for density control).

References

- [1] K. H. Bhatt, S. Grego, O. D. Velev, *Langmuir* **2005**, *21*, 6603.
- [2] J. Oh, R. Hart, J. Capurro, H. M. Noh, *Lab Chip* **2009**, *9*, 62.
- [3] E. M. Melvin, B. R. Moore, K. H. Gilchrist, S. Grego, O. D. Velev, *Biomicrofluidics* **2011**, *5*, 34113.
- [4] R. Xie, X.-Y. Liu, *Adv. Funct. Mater.* **2008**, *18*, 802.
- [5] Y. Kung, K. Huang, W. Chong, P. Chiou, *Small* **2016**, *12*, 4343.
- [6] H. Huang, H. D. Ou-Yang, *Electrophoresis* **2017**, *38*, 1609-1616.